Inorganic Chemistry

Article

pubs.acs.org/IC

New Polymorphs of Ternary Sodium Tellurium Oxides: Hydrothermal Synthesis, Structure Determination, and Characterization of β-$Na_2Te_4O_9$ and $Na_2Te_2O_6{\cdot}1.5H_2O$

Dong Woo Lee and Kang Min Ok*

Department of Chemistry, Chung-Ang University, 84 Heukseok-ro, Dongjak-gu, Seoul 156-756, Republic of Korea

Supporting Information

ABSTRACT: Two new sodium tellurium oxide materials, β-$Na_2Te_4O_9$ and $Na_2Te_2O_6{\cdot}1.5H_2O$, have been synthesized through hydrothermal reactions using Na_2CO_3, TeO_2, and $H_2TeO_4{\cdot}2H_2O$ as reagents. The structures of the novel materials have been determined by single crystal X-ray diffraction. β-$Na_2Te_4O_9$ is a new polymorph of ternary tellurite that is showing a three-dimensional framework structure containing only TeO_4 polyhedra. $Na_2Te_2O_6{\cdot}1.5H_2O$ reveals an anionic layered backbone composed of $Te^{6+}O_6$ octahedra and $Te^{4+}O_5$ polyhedra. Thermogravimetric analyses and powder X-ray diffractions at different temperatures suggest that the frameworks of β-$Na_2Te_4O_9$ and $Na_2Te_2O_6{\cdot}1.5H_2O$ are thermally stable up to 480 and 400 °C, respectively. The Na^+ cations in between the anionic layers in $Na_2Te_2O_6{\cdot}1.5H_2O$ are completely replaced by Li^+ cations through an ion-exchange reaction. The UV−vis diffuse reflectance and infrared spectra, elemental analyses, and local dipole moment calculations are also reported.

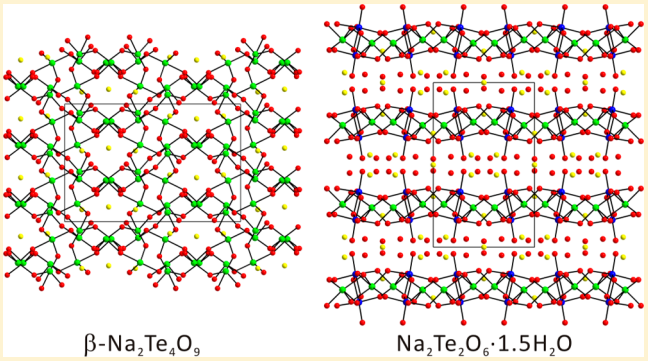

INTRODUCTION

Tellurites, i.e., oxide materials containing Te^{4+} cations, have been of particular interest in broad inorganic solid-state chemistry field. For the synthesis of tellurite materials, tellurium dioxide (TeO_2) has been most frequently introduced as a starting material, which may be attributed to its excellent reactivity with most oxide reagents, relatively lower melting point (733 °C) as an oxide, effectiveness as a flux to grow crystals, and extraordinary solubility in various solvents under mild reaction conditions.[1−5] Structurally, tellurites crystallizing in extended structures such as 1-D chains, 2-D layers, and 3-D frameworks often exhibit rich structural chemistry.[6−10] In fact, the structural diversity of tellurites originates from a variety of coordination modes of Te^{4+} cations such as TeO_3 trigonal pyramids, TeO_4 seesaws, and TeO_5 square pyramids. Moreover, as an important second-order Jahn−Teller (SOJT) distortive cation,[11−15] the Te^{4+} cation can show an asymmetric coordination mode attributable to the stereoactive lone pair on it. When the local asymmetric unit is aligned in a parallel manner within extended structures, macroscopic noncentrosymmetric (NCS) materials with very interesting materials' properties such as pyroelectricity, ferroelectricity, piezoelectricity, and second-harmonic generation (SHG) have been readily found.[16−21] Thus, many synthetic chemists have made continuous efforts to discover enhanced NCS mixed metal tellurites.[22−29] However, it should be noted that currently discovering new ternary tellurites, namely, oxide materials composed of Te^{4+} and only one more metal cation, is extremely difficult, since the majority of ternary tellurites have been already discovered. Among many, we have been interested in investigating new ternary tellurites in the Na^+−Te^{4+}−oxide system. Until now, several ternary sodium tellurites and tellurite hydrates such as Na_2TeO_3,[30] $Na_2TeO_3{\cdot}5H_2O$,[31] $Na_2Te_2O_5{\cdot}2H_2O$,[32] α-$Na_2Te_4O_9$,[33] and $Na_4Te_4O_{10}$[34] exhibiting various structural characteristics have been reported. During the exploratory hydrothermal syntheses reactions, we were able to discover a new polymorph of ternary tellurite, β-$Na_2Te_4O_9$, and a mixed-valent tellurite-tellurate, $Na_2Te_2O_6{\cdot}1.5H_2O$. Here, we present phase pure synthesis, detailed structural analysis, and complete characterization of two novel sodium tellurium oxide materials. With $Na_2Te_2O_6{\cdot}1.5H_2O$, a robust ion-exchange behavior will also be introduced.

EXPERIMENTAL SECTION

Reagents. Na_2CO_3 (Aldrich, 99.5%), TeO_2 (Alfa Aesar, 98%), and $H_2TeO_4{\cdot}2H_2O$ (Alfa Aesar, 99%) were used as received.

Synthesis. Hydrothermal reactions were utilized to synthesize pure phases of the reported materials. For β-$Na_2Te_4O_9$, a 0.212 g portion (2.00×10^{-3} mol) of Na_2CO_3, 0.319 g (2.00×10^{-3} mol) of TeO_2, and 0.5 mL of deionized water were combined. With $Na_2Te_2O_6{\cdot}1.5H_2O$, a 0.158 g portion ($1.50 \times 10^{-3}$ mol) of Na_2CO_3, 0.159 g (1.00×10^{-3} mol) of TeO_2, 0.230 g (1.00×10^{-3} mol) of $H_2TeO_4{\cdot}2H_2O$, and 1 mL of deionized water were combined. Each of the reaction mixtures was placed in a Teflon-lined (23 mL) stainless steel autoclave and tightly sealed. The autoclaves were slowly heated to 230 °C, held for 4 days, and cooled to room temperature at a rate of 6 °C h^{-1}. After cooling, the reactors were opened, and the products

Received: July 19, 2014
Published: September 11, 2014

dx.doi.org/10.1021/ic501739u | Inorg. Chem. 2014, 53, 10642−10648

were isolated by filtration. After washing with distilled water several times, the products were dried overnight at room temperature. Colorless crystals of β-$Na_2Te_4O_9$ and $Na_2Te_2O_6{\cdot}1.5H_2O$ were obtained in 53% and 43% yields, respectively, based on Na_2CO_3.

Single Crystal X-ray Diffraction. Crystal structures of β-$Na_2Te_4O_9$ and $Na_2Te_2O_6{\cdot}1.5H_2O$ were determined by a standard crystallographic method. A colorless block crystal (0.022 × 0.025 × 0.032 mm^3) of β-$Na_2Te_4O_9$ and a colorless block crystal (0.022 × 0.025 × 0.036 mm^3) of $Na_2Te_2O_6{\cdot}1.5H_2O$ were selected for single crystal X-ray diffraction analyses. Diffraction data were collected at room temperature using a Bruker SMART BREEZE diffractometer equipped with a 1K CCD area detector using graphite monochromated Mo Kα radiation. A narrow-frame method was used with an exposure time of 10 s/frame, and scan widths of 0.30° in ω to collect a hemisphere of data. The first 50 frames were remeasured at the end of the data collection to monitor crystal and instrument stability. The maximum correction applied to the intensities was <1%. The data were integrated using the SAINT program,[35] with the intensities corrected for polarization, Lorentz factor, air absorption, and absorption attributed to the variation in the path length through the detector faceplate. A semiempirical absorption correction was made on the hemisphere of data with the SADABS program.[36] The data were solved using SHELXS-97[37] and refined with SHELXL-97.[38] All calculations were performed using the WinGX-98 crystallographic software package.[39] Crystallographic data and selected bond distances for β-$Na_2Te_4O_9$ and $Na_2Te_2O_6{\cdot}1.5H_2O$ are listed in Tables 1 and 2, respectively.

Table 1. Crystallographic Data for β-$Na_2Te_4O_9$ and $Na_2Te_2O_6{\cdot}1.5H_2O$

formula	$Na_2Te_4O_9$	$Na_4Te_4O_{15}H_6$
fw	700.38	848.36
space group	*Pccn* (No. 56)	*C*2/*c* (No. 15)
a (Å)	16.317(2)	8.9884(19)
b (Å)	10.4544(10)	14.3739(19)
c (Å)	10.8874(10)	10.387(3)
β (deg)	90	99.429(11)
V (Å^3)	1857.2(3)	1323.9(5)
Z	8	4
T (K)	298.0(2)	298.0(2)
λ (Å)	0.710 73	0.710 73
$R(F)^a$	0.0229	0.0259
$R_w(F_o^2)^b$	0.0489	0.0394

$^aR(F) = \Sigma||F_o| - |F_c||/\Sigma|F_o|$. $^bR_w(F_o^2) = [\Sigma w(F_o^2 - F_c^2)^2/\Sigma w(F_o^2)^2]^{1/2}$.

Powder X-ray Diffraction (PXRD). PXRD was used to confirm the phase purity of the newly synthesized materials. The data were obtained on a Bruker D8-Advance diffractometer using Cu Kα radiation at room temperature with 40 kV and 40 mA. The polycrystalline samples of β-$Na_2Te_4O_9$ and $Na_2Te_2O_6{\cdot}1.5H_2O$ were mounted on sample holders and scanned in the 2θ range 5−70° with a step size of 0.02° and a step time of 0.2 s. The measured PXRD data are in very good agreement with the calculated patterns from the single crystal models (see the Supporting Information).

Infrared (IR) Spectroscopy. IR spectra were recorded on a Nicolet 6700 FT-IR spectrometer in the 400−4000 cm^{-1} range, with the samples embedded in KBr matrices.

UV−Vis Diffuse Reflectance Spectroscopy. UV−vis diffuse reflectance spectral data for β-$Na_2Te_4O_9$ and $Na_2Te_2O_6{\cdot}1.5H_2O$ were obtained at room temperature on a Varian Cary 500 scan UV−vis−NIR spectrophotometer with a double-beam photomultiplier tube in the spectral range 200−2500 nm at the Korea Photonics Technology Institute. The reflectance spectra were converted into the absorbance data using the Kubelka−Munk function.[40,41]

Thermogravimetric Analysis (TGA). TGA was performed on a Setaram LABSYS TG-DTA thermogravimetric analyzer. The polycrystalline samples for both reported materials were contained within alumina crucibles and heated at a rate of 10 °C min^{-1} from room temperature to 1000 °C under flowing argon.

Scanning Electron Microscopy/Energy Dispersive Analysis by X-ray (SEM/EDAX). SEM/EDAX has been performed using a Hitachi S-3400N and a Horiba Energy EX-250 instrument. EDAX data for β-$Na_2Te_4O_9$ and $Na_2Te_2O_6{\cdot}1.5H_2O$ reveal Na:Te ratios of 1.0:2.0 and 1.1:1.0, respectively.

Ion-Exchange Experiments. To perform ion-exchange reactions, ca. 150 mg of polycrystalline $Na_2Te_2O_6{\cdot}1.5H_2O$ was stirred in 5 mL of 2 M $LiNO_3$(aq) solutions at 50 °C for 5 days. After that, the product was isolated by filtration, thoroughly washed with excess water, and dried overnight in air.

Inductively Coupled Plasma-Optical Emission Spectroscopy (ICP-OES) Analysis. The composition of the ion-exchanged solid was determined by ICP-OES analysis using a PerkinElmer Optima 8300 instrument.

RESULTS AND DISCUSSION

Structure. β-$Na_2Te_4O_9$. β-$Na_2Te_4O_9$ is a new polymorph of ternary tellurite crystallizing in a centrosymmetric orthorhombic space group, *Pccn* (No. 56). Whereas crystals of α-$Na_2Te_4O_9$[33] were obtained through a solid-state reaction between stoichiometric amounts of TeO_2 and Na_2CO_3 at 750 °C, those of β-$Na_2Te_4O_9$ were grown through a hydrothermal reaction at 230 °C. The framework of β-$Na_2Te_4O_9$ consists of only TeO_4 polyhedra with Te−O−Te bonds. There are four unique Te^{4+} cations in an asymmetric unit, and all four Te^{4+} cations are linked to four oxygen atoms in unsymmetrical coordination environments attributable to their stereoactive lone pairs (see Figure 1). While three of the Te^{4+} cations, i.e., $Te(1)^{4+}$, $Te(2)^{4+}$, and $Te(3)^{4+}$, reveal two normal [1.818(3)−1.925(3) Å] and two long [2.031(3)−2.182(3) Å] Te−O bond distances, the $Te(4)^{4+}$ exhibits three normal [1.815(3)−1.977(3) Å] and one very long [2.402(3) Å] Te−O bond lengths. The O−Te−O bond angles

Table 2. Selected Bond Distances (Å) for β-$Na_2Te_4O_9$ and $Na_2Te_2O_6{\cdot}1.5H_2O$

β-$Na_2Te_4O_9$				$Na_2Te_2O_6{\cdot}1.5H_2O$	
Te(1)−O(1)	1.865(3)	Te(3)−O(2)	1.925(3)	Te(1)−O(1)	1.834(3)
Te(1)−O(2)	2.099(3)	Te(3)−O(5)	2.177(3)	Te(1)−O(2)	1.893(3)
Te(1)−O(3)	2.125(3)	Te(3)−O(7)	1.818(3)	Te(1)−O(3)	1.917(3)
Te(1)−O(4)	1.880(3)	Te(3)−O(8)	2.031(3)	Te(1)−O(4)	1.966(3)
Te(2)−O(1)	2.182(3)	Te(4)−O(3)	1.904(3)	Te(1)−O(5)	1.994(3)
Te(2)−O(4)	2.128(3)	Te(4)−O(6)	2.402(3)	Te(1)−O(5)	1.997(3)
Te(2)−O(5)	1.887(3)	Te(4)−O(8)	1.977(3)	Te(2)−O(2)	2.119(3)
Te(2)−O(6)	1.835(3)	Te(4)−O(9)	1.815(3)	Te(2)−O(3)	2.108(3)
				Te(2)−O(4)	1.971(3)
				Te(2)−O(6)	1.859(3)
				Te(2)−O(6)	2.413(3)

dx.doi.org/10.1021/ic501739u | *Inorg. Chem.* 2014, 53, 10642−10648

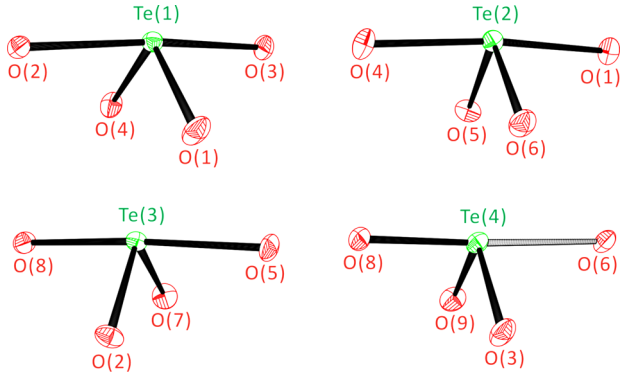

Figure 1. ORTEP (50% probability ellipsoids) drawings of TeO_4 polyhedra in β-$Na_2Te_4O_9$.

in TeO_4 polyhedra range from 84.75(13)° to 175.34(13)°. Among three unique Na^+ cations, $Na(1)^+$ and $Na(2)^+$ interact with six oxygen atoms, whereas $Na(3)^+$ contacts with seven oxygen atoms. The Na−O contact distances range from 2.259(4) to 2.781(4) Å. The $Te(1)O_4$, $Te(2)O_4$, and $Te(3)O_4$ polyhedra share their corners through O(1), O(2), and O(5) and form a Te_3O_8 cyclic trimer (see Figure 2a). As seen in Figure 2a,b, each Te_3O_8 cyclic trimer further shares O(4) and generates infinite helical chains that run through the [001] direction. And then, the $Te(4)O_4$ polyhedra link the helical chains through O(3), O(6), and O(9) along the [100] direction and form a three-dimensional framework (see Figure 2c). The very long Te(4)−O(6) bond distance [2.402(3) Å] observed from $Te(4)O_4$ linkers may be attributed to the chain propagation along the [001] direction. As can be seen in Figure 2c, Na^+ cations reside in channels running down to the [010] direction. In connectivity terms, the structure of β-$Na_2Te_4O_9$ can be described as an anionic framework of $\{[Te(1)O_{4/2}]^0[Te(2)O_{4/2}]^0[Te(3)O_{3/2}O_{1/1}]^{1-}[Te(4)O_{3/2}O_{1/1}]^{1-}\}^{2-}$, and charge balance is maintained by the incorporation of the Na^+ cations. Bond valence sum calculations[42,43] for the Na^+ and Te^{4+} result in values of 0.91−1.14 and 3.96−4.05, respectively. Although α-$Na_2Te_4O_9$ and β-$Na_2Te_4O_9$ are stoichiometrically identical, they do exhibit quite different structural characteristics. While the backbone of α-$Na_2Te_4O_9$ is composed of both TeO_4 and TeO_5 units, the framework of β-$Na_2Te_4O_9$ consists of only TeO_4 polyhedra (see the Supporting Information). In addition, the structure of α-$Na_2Te_4O_9$ shows unidimensional polymeric sheets that are composed of Te_4O_9 units, whereas that of β-$Na_2Te_4O_9$ reveals a three-dimensional framework composed of TeO_4 polyhedra.

$Na_2Te_2O_6{\cdot}1.5H_2O$. $Na_2Te_2O_6{\cdot}1.5H_2O$ is a new mixed-valent alkali metal tellurite−tellurate hydrate ($Na_2Te^{4+}Te^{6+}O_6{\cdot}1.5H_2O$) that crystallizes in the monoclinic space group, $C2/c$ (No. 15). The material exhibits a novel layered structure, and each layer consists of both TeO_6 and TeO_5 polyhedra (see Figure 3). While the $Te(1)^{6+}$ cation is linked to six oxygen atoms in an octahedral coordination environment, the $Te(2)^{4+}$ cation is connected to five oxygen atoms in an asymmetric TeO_5 coordination mode attributed to the stereoactive lone pair. The observed Te^{6+}−O bond distances range from 1.834(3) to 1.997(3) Å, whereas the Te^{4+}−O bond lengths range from 1.859(3) to 2.413(3) Å. Three unique Na^+ cations existing within an asymmetric unit interact with oxygen atoms in oxide ligands as well as in disordered water molecules. The Na^+−O contact distances range from 2.244(4) to 3.000(3) Å. Two $Te(1)^{6+}O_6$ octahedra share their edges through two O(5) and form $Te(1)^{6+}{}_2O_{10}$ dimers (see Figure 4a). Also, as seen in Figure 4a, two $Te(2)^{4+}O_5$ polyhedra share their own edges through two O(6), which results in $Te(2)^{4+}{}_2O_8$ dimers. Then, $Te(1)^{6+}{}_2O_{10}$ and $Te(2)^{4+}{}_2O_8$ dimers further share their corners and edges through O(1), O(2), and O(4) and complete a novel layer in the *ac*-plane. Interestingly, four-membered rings (4-MRs) and six-membered rings (6-MRs) are observed from the layer. Lone pairs on Te^{4+} cations reside within the 4-MRs, and they point toward approximately [001] and [00−1] directions. Na^+ cations and disordered water molecules reside in between the layers and complete the two-dimensional structure of $Na_2Te_2O_6{\cdot}1.5H_2O$ (see Figure 4b). As seen in Figure 4c, slightly corrugated layers composed of $Te^{6+}O_6$ and $Te^{4+}O_5$ polyhedra are also observed along the [100] direction. The structure of $Na_2Te_2O_6{\cdot}1.5H_2O$ may be described as an anionic layer of $\{[Te(1)^{6+}O_{5/2}O_{1/1}]^{1-}[Te(2)^{4+}O_{5/2}]^{1-}\}^{2-}$ and the Na^+ cations residing in between the layers retain the charge balance. Bond valence sum calculations[42,43] for the Na^+, Te^{6+}, and Te^{4+} result in values of 0.97−1.15, 5.87, and 4.05, respectively.

IR Spectroscopy. The IR spectra of β-$Na_2Te_4O_9$ and $Na_2Te_2O_6{\cdot}1.5H_2O$ reveal characteristic Te−O vibrations at ca. 631−815 and 421−571 cm^{-1}. For $Na_2Te_2O_6{\cdot}1.5H_2O$, vibrations attributable to H_2O molecules are also observed at ca. 1651 and 3330−3604 cm^{-1}. The assignments agreed well with those for previously reported tellurium oxides materials.[44−48] The IR spectra for the reported materials are given in the Supporting Information.

UV−Vis Diffuse Reflectance Spectroscopy. UV−vis diffuse reflectance spectra for β-$Na_2Te_4O_9$ and $Na_2Te_2O_6{\cdot}1.5H_2O$ were obtained, and the absorption (K/S) data were calculated from the following Kubelka−Munk function:[40,41]

$$F(R) = \frac{(1-R)^2}{2R} = \frac{K}{S}$$

Here, K is the absorption, S is the scattering, and R is the reflectance. In the (K/S)-versus-E plots, extrapolating the linear part of the rising curve to zero resulted in the onset of absorptions at 3.3 and 3.4 eV for β-$Na_2Te_4O_9$ and $Na_2Te_2O_6{\cdot}1.5H_2O$, respectively (see Figure 5). The band gaps for the reported materials may be mainly attributable to the interactions of Te−O bonds as well as the distortions that originate from TeO_4 and TeO_5 polyhedra.

Thermal Analysis. TGA was employed to examine the thermal behaviors of β-$Na_2Te_4O_9$ and $Na_2Te_2O_6{\cdot}1.5H_2O$. No significant weight loss is observed from the TGA diagram of β-$Na_2Te_4O_9$ up to 920 °C. However, an endothermic peak occurs in the heating curve of the differential thermal analysis (DTA) data at about 480 °C, which might be attributable to the incongruent melting of the material. In order to confirm the thermal behavior, PXRD measurements at different temperatures were performed. The PXRD patterns reveal that the material maintains the crystallinity up to 450 °C. However, the pattern obtained at 500 °C shows that β-$Na_2Te_4O_9$ starts decomposing and collapsing to an amorphous phase by 1000 °C. With $Na_2Te_2O_6{\cdot}1.5H_2O$, loss of hydrated water molecules is observed to 260 °C with a weight loss of 5.43% (calcd 6.37%). Although no weight loss is monitored from the TGA diagram up to 600 °C, endothermic peaks appear at 400 °C in the DTA diagram. PXRD patterns measured at higher temperatures suggest that the dehydrated material exhibits crystallinity with similar framework structure to that of starting material to 400 °C. Above the temperature, the material decomposes to the mixture of Te_2O_5 (PDF: 71-0508) and some amorphous phases. Thus, the endothermic peaks found at ca. 640 and 700 °C in the DTA data may be

dx.doi.org/10.1021/ic501739u | Inorg. Chem. 2014, 53, 10642−10648

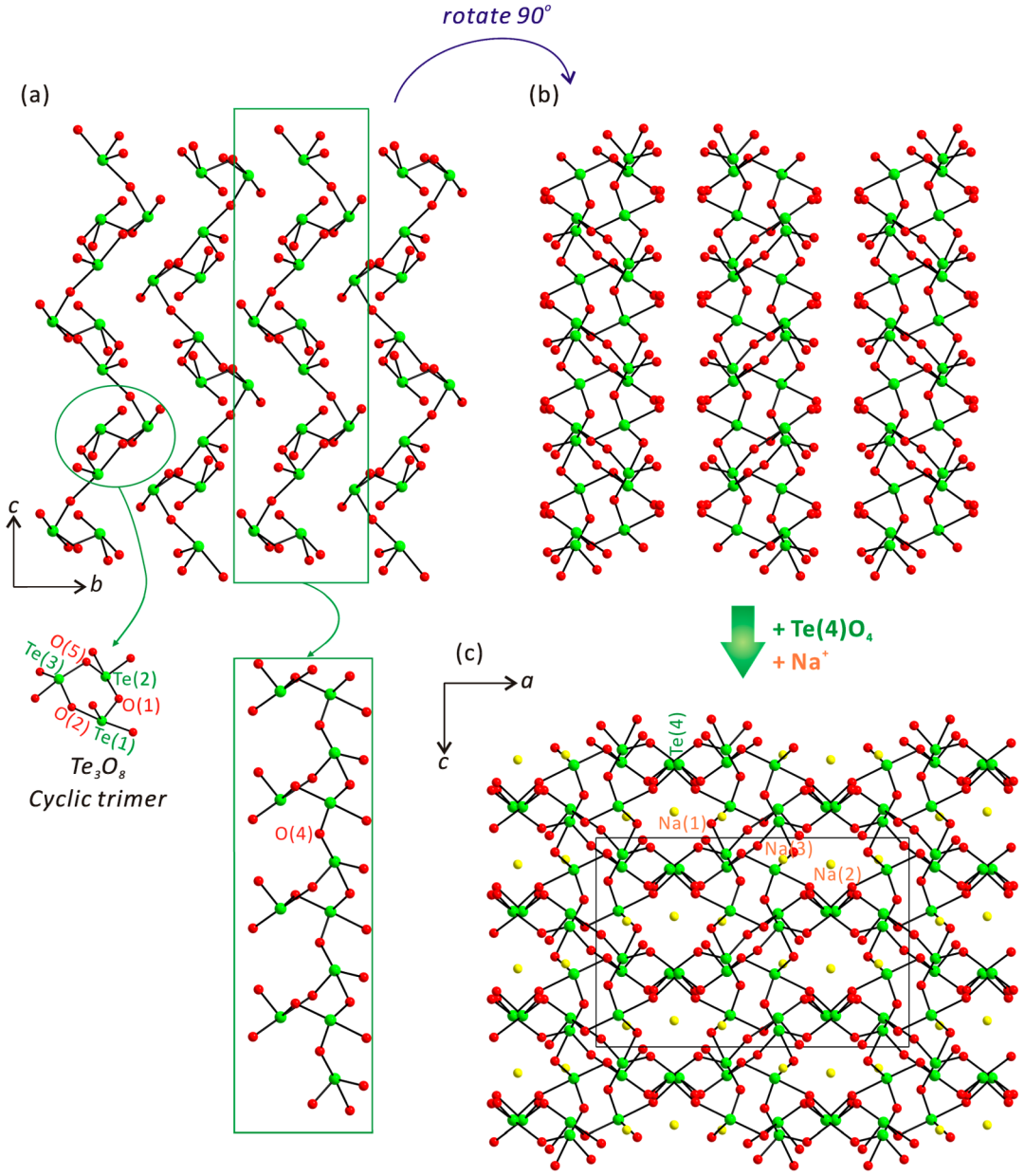

Figure 2. Ball-and-stick representations of chains containing Te_3O_8 cyclic trimers in the (a) *bc*-plane and (b) *ac*-plane in β-$Na_2Te_4O_9$. (c) A three-dimensional framework is completed by the linking of $Te(4)O_4$ polyhedra and Na^+ cations (yellow, Na; green, Te; red, O).

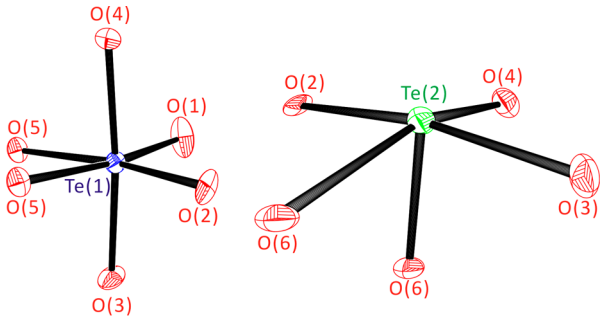

Figure 3. ORTEP (50% probability ellipsoids) drawings of $Te(1)^{6+}O_6$ and $Te(2)^{4+}O_5$ polyhedra in $Na_2Te_2O_6{\cdot}1.5H_2O$.

attributed to the decomposition and phase transition. The TGA diagrams and PXRD data obtained at different temperatures are shown in the Supporting Information.

Ion-Exchange Experiments. As we discussed earlier, $Na_2Te_2O_6{\cdot}1.5H_2O$ exhibits a layered structure, and Na^+ cations reside in between the anionic layers to make a charge balance. Thus, we thought that the Na^+ could be replaced by Li^+ through ion-exchange reactions. A suspension of $Na_2Te_2O_6{\cdot}1.5H_2O$ was stirred in a ~2 M solution of $LiNO_3$ for 5 days at 50 °C. It was possible to replace the Na^+ cation completely for Li^+. The PXRD pattern for the isolated product reveals a very high crystallinity, and the unit-cell parameters for the ion-exchanged material may be indexed on a triclinic cell with $a \sim 7.85$ Å, $b \sim 7.82$ Å, $c \sim 6.75$ Å, $\alpha \sim 105.1°$, $\beta \sim 90.9°$, and $\gamma \sim 87.9°$ (see Figure 6). To determine the crystal structure of the new phase, a full ab initio structural determination is in progress. Since the PXRD pattern of the Li^+-exchanged material does not match any known compounds, the ion-exchange reactions of the layered $Na_2Te_2O_6{\cdot}1.5H_2O$ may provide an easy synthetic method for the preparation of new layered materials under mild conditions.

dx.doi.org/10.1021/ic501739u | *Inorg. Chem.* 2014, 53, 10642−10648

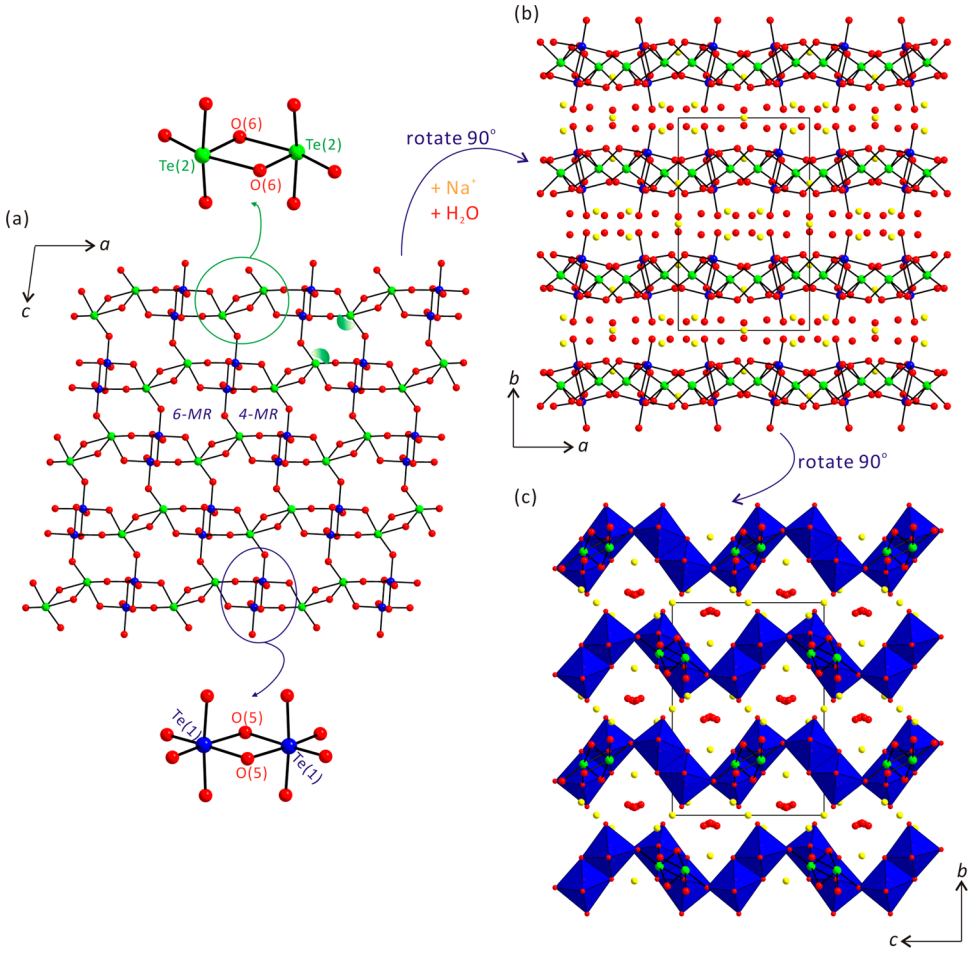

Figure 4. Ball-and-stick and polyhedral representations of (a) a layer in the *ac*-plane and completed layers with Na^+ cations and disordered water molecules in the (b) *ab*-plane and (c) *bc*-plane in $Na_2Te_2O_6{\cdot}1.5H_2O$ (yellow, Na; blue, Te^{6+}; green, Te^{4+}; red, O).

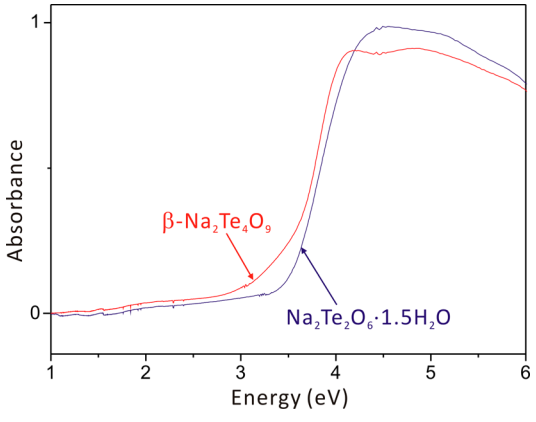

Figure 5. UV–vis diffuse reflectance spectra of β-$Na_2Te_4O_9$ and $Na_2Te_2O_6{\cdot}1.5H_2O$ exhibiting the absorption edges at 3.3 and 3.4 eV, respectively.

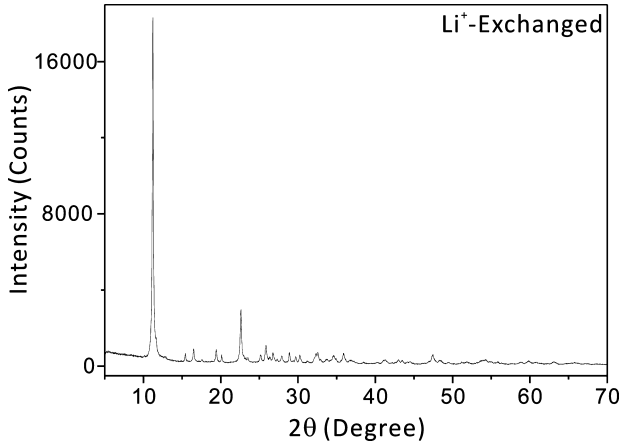

Figure 6. Powder X-ray diffraction pattern (Cu Kα radiation) of the product of the ion-exchange of $Na_2Te_2O_6{\cdot}1.5H_2O$ with Li^+ cation. The pattern can be indexed on a triclinic unit cell with $a \sim 7.85$ Å, $b \sim 7.82$ Å, $c \sim 6.75$ Å, $\alpha \sim 105.1°$, $\beta \sim 90.9°$, and $\gamma \sim 87.9°$.

Dipole Moment Calculations. β-$Na_2Te_4O_9$ and $Na_2Te_2O_6{\cdot}1.5H_2O$ contain polyhedra of asymmetric coordination environment, i.e., TeO_4 and TeO_5 attributable to the stereoactive lone pairs, although both of the materials crystallize in macroscopic centrosymmetric space groups. It is, however, worthwhile to quantify the extent of distortions for the local asymmetric polyhedra in order to better understand the extended asymmetric frameworks. A convenient method to quantify the asymmetric environment is calculating the local dipole moments for the constituent polyhedra using a bond valence sum approach.[49−51] By using this method, the calculated local dipole moments for TeO_4 and TeO_5 polyhedra in β-$Na_2Te_4O_9$ and $Na_2Te_2O_6{\cdot}1.5H_2O$ are about 6.2−8.4 and 8.7 D (Debyes), respectively. The dipole moments are similar to those of TeO_4 and TeO_5 polyhedra found from previously reported

dx.doi.org/10.1021/ic501739u | Inorg. Chem. 2014, 53, 10642−10648

Table 3. Calculation of Dipole Moments for TeO_4 and TeO_5 Polyhedra in β-$Na_2Te_4O_9$ and $Na_2Te_2O_6{\cdot}1.5H_2O$ (D = Debyes)

species	dipole moment (D)
$Te(1)O_4$	8.4
$Te(2)O_4$	6.2
$Te(3)O_4$	7.1
$Te(4)O_4$	8.1
$Te(1)O_5$	8.7

tellurites.[10,47,48,52,53] The local dipole moments for TeO_4 and TeO_5 groups are listed in Table 3.

CONCLUSIONS

Pure phases of two novel sodium tellurium oxide materials, β-$Na_2Te_4O_9$ and $Na_2Te_2O_6{\cdot}1.5H_2O$, have been hydrothermally synthesized, and the structures were determined by a standard crystallographic method using X-ray diffraction. While the new polymorph of ternary tellurite, β-$Na_2Te_4O_9$, reveals a three-dimensional framework consisting of only TeO_4 polyhedra, the mixed-valent sodium tellurite–tellurate, $Na_2Te_2O_6{\cdot}1.5H_2O$, exhibits a layered structure composed of TeO_6 and TeO_5 polyhedra. UV–vis diffuse reflectance spectra suggest that β-$Na_2Te_4O_9$ and $Na_2Te_2O_6{\cdot}1.5H_2O$ have band gaps of 3.3 and 3.4 eV, respectively. $Na_2Te_2O_6{\cdot}1.5H_2O$ displayed a robust ion-exchange behavior, and the Na^+ cation was completely replaced by the Li^+ cation. The ion-exchange capability of the $Na_2Te_2O_6{\cdot}1.5H_2O$ provides a facile way for the mild synthesis of new layered materials.

ASSOCIATED CONTENT

Supporting Information

X-ray crystallographic files in CIF format, calculated and observed X-ray diffraction patterns, IR spectra, and thermogravimetric analysis diagrams for β-$Na_2Te_4O_9$ and $Na_2Te_2O_6{\cdot}1.5H_2O$. This material is available free of charge via the Internet at http://pubs.acs.org.

AUTHOR INFORMATION

Corresponding Author

*E-mail: kmok@cau.ac.kr. Phone: +82-2-820-5197. Fax: +82-2-825-4736.

Notes

The authors declare no competing financial interest.

ACKNOWLEDGMENTS

This research was supported by the Basic Science Research Program through the National Research Foundation of Korea (NRF) funded by Ministry of Education, Science & Technology (Grant 2013R1A2A2A01007170).

REFERENCES

(1) Alonso, J. A.; Castro, A.; Puebla, E. G.; Monge, M. A.; Rasines, I.; Valero, C. R. *J. Solid State Chem.* **1987**, *69*, 36–42.
(2) Champarnaud-Mesjard, J. C.; Frit, B.; Chagraoui, A.; Tairi, A. *J. Solid State Chem.* **1996**, *127*, 248–255.
(3) Ok, K. M.; Orzechowski, J.; Halasyamani, P. S. *Inorg. Chem.* **2004**, *43*, 964–968.
(4) Lide, D. R. *CRC Handbook of Chemistry and Physics, Internet Version 2005*; CRC Press: Boca Raton, FL, 2005.
(5) Zhang, Z.; Tao, X.; Zhang, J.; Sun, Y.; Zhang, C.; Li, B. *CrystEngComm* **2013**, *15*, 10197–10204.
(6) Alcock, N. W.; Harrison, W. D. *Acta Crystallogr.* **1982**, *B38*, 1809–1811.
(7) Mayer, H.; Weil, M. *Z. Anorg. Allg. Chem.* **2003**, *629*, 1068–1072.
(8) Kong, F.; Hu, C.; Hu, T.; Zhou, Y.; Mao, J.-G. *Dalton Trans.* **2009**, 4962–4970.
(9) Kim, M. K.; Kim, S.-H.; Chang, H.-Y.; Halasyamani, P. S.; Ok, K. M. *Inorg. Chem.* **2010**, *49*, 7028–7034.
(10) Kim, Y. H.; Lee, D. W.; Ok, K. M. *Inorg. Chem.* **2014**, *53*, 5240–5245.
(11) Opik, U.; Pryce, M. H. L. *Proc. R. Soc. London* **1957**, *A238*, 425–447.
(12) Bader, R. F. W. *Can. J. Chem.* **1962**, *40*, 1164–1175.
(13) Pearson, R. G. *J. Am. Chem. Soc.* **1969**, *91*, 4947–4955.
(14) Pearson, R. G. *THEOCHEM* **1983**, *103*, 25–34.
(15) Wheeler, R. A.; Whangbo, M.-H.; Hughbanks, T.; Hoffmann, R.; Burdett, J. K.; Albright, T. A. *J. Am. Chem. Soc.* **1986**, *108*, 2222–2236.
(16) Nye, J. F. *Physical Properties of Crystals*; Oxford University Press: Oxford, 1957.
(17) Jona, F.; Shirane, G. *Ferroelectric Crystals*; Pergamon Press: Oxford, 1962.
(18) Cady, W. G. *Piezoelectricity; An Introduction to the Theory and Applications of Electromechanical Phenomena in Crystals*; Dover: New York, 1964; p 822.
(19) Lang, S. B. *Sourcebook of Pyroelectricity*; Gordon & Breach Science: London, 1974.
(20) Halasyamani, P. S.; Poeppelmeier, K. R. *Chem. Mater.* **1998**, *10*, 2753–2769.
(21) Ok, K. M.; Chi, E. O.; Halasyamani, P. S. *Chem. Soc. Rev.* **2006**, *35*, 710–717.
(22) Balraj, V.; Vidyasagar, K. *Inorg. Chem.* **1998**, *37*, 4764–4774.
(23) Almond, P. M.; McKee, M. L.; Albrecht-Schmitt, T. E. *Angew. Chem., Int. Ed.* **2002**, *41*, 3426–3429.
(24) Goodey, J.; Broussard, J.; Halasyamani, P. S. *Chem. Mater.* **2002**, *14*, 3174–3180.
(25) Ra, H.-S.; Ok, K. M.; Halasyamani, P. S. *J. Am. Chem. Soc.* **2003**, *125*, 7764–7765.
(26) Chi, E. O.; Ok, K. M.; Porter, Y.; Halasyamani, P. S. *Chem. Mater.* **2006**, *18*, 2070–2074.
(27) Zhang, S.; Jiang, H.; Sun, C.; Mao, J.-G. *Inorg. Chem.* **2009**, *48*, 11809–11820.
(28) Kong, F.; Xu, X.; Mao, J.-G. *Inorg. Chem.* **2010**, *49*, 11573–11580.
(29) Zhang, S.-Y.; Hu, C.-L.; Li, P.-X.; Jiang, H.-L.; Mao, J.-G. *Dalton Trans.* **2012**, *41*, 9532–9542.
(30) Masse, R.; Guitel, J. C.; Trodjman, I. *Mater. Res. Bull.* **1980**, *15*, 431–436.
(31) Philippot, E.; Maurin, M.; Moret, J. *Acta Crystallogr., Sect. B* **1979**, *35*, 1337–1340.
(32) Daniel, F.; Moret, J.; Maurin, M.; Philippot, E. *Acta Crystallogr., Sect. B* **1981**, *B37*, 1278–1281.
(33) Tagg, S. L.; Huffman, J. C.; Zwanziger, J. W. *Chem. Mater.* **1994**, *6*, 1884–1889.
(34) Tagg, S. L.; Huffman, J. C.; Zwanziger, J. W. *Acta Chem. Scand.* **1997**, *51*, 118–121.
(35) *SAINT, Program for Area Detector Absorption Correction, version 4.05*; Siemens Analytical X-ray Instruments: Madison, WI, 1995.
(36) Blessing, R. H. *Acta Crystallogr., Sect. A* **1995**, *A51*, 33–38.
(37) Sheldrick, G. M. *SHELXS-97—A Program for Automatic Solution of Crystal Structures*; University of Goettingen: Goettingen, Germany, 1997.
(38) Sheldrick, G. M. *SHELXL-97—A Program for Crystal Structure Refinement*; University of Goettingen: Goettingen, Germany, 1997.
(39) Farrugia, L. J. *J. Appl. Crystallogr.* **1999**, *32*, 837–838.
(40) Kubelka, P.; Munk, F. *Z. Technol. Phys.* **1931**, *12*, 593.
(41) Tauc, J. *Mater. Res. Bull.* **1970**, *5*, 721–729.
(42) Brown, I. D.; Altermatt, D. *Acta Crystallogr.* **1985**, *B41*, 244–247.
(43) Brese, N. E.; O'Keeffe, M. *Acta Crystallogr.* **1991**, *B47*, 192–197.

(44) Ok, K. M.; Halasyamani, P. S. *Inorg. Chem.* **2005**, *44*, 3919−3925.
(45) Jiang, H.; Xie, Z.; Mao, J.-G. *Inorg. Chem.* **2007**, *46*, 6495.
(46) Gu, Q.-H.; Hu, C.-L.; Zhang, J.-H.; Mao, J.-G. *Dalton Trans.* **2011**, *40*, 2562−2569.
(47) Lee, D. W.; Oh, S.-J.; Halasyamani, P. S.; Ok, K. M. *Inorg. Chem.* **2011**, *50*, 4473−4480.
(48) Kim, Y. H.; Lee, D. W.; Ok, K. M. *Inorg. Chem.* **2014**, *53*, 1250−1256.
(49) Galy, J.; Meunier, G. *J. Solid State Chem.* **1975**, *13*, 142−159.
(50) Maggard, P. A.; Nault, T. S.; Stern, C. L.; Poeppelmeier, K. R. *J. Solid State Chem.* **2003**, *175*, 27−33.
(51) Izumi, H. K.; Kirsch, J. E.; Stern, C. L.; Poeppelmeier, K. R. *Inorg. Chem.* **2005**, *44*, 884−895.
(52) Kim, M. K.; Jo, V.; Lee, D. W.; Ok, K. M. *Dalton Trans.* **2010**, *39*, 6037−6042.
(53) Kim, Y. H.; Lee, D. W.; Ok, K. M. *Inorg. Chem.* **2013**, *52*, 11450−11456.